

K-Bayes Reconstruction for Perfusion MRI I: Concepts and Application

John Kornak,^{1,2} Karl Young,^{1,3} Norbert Schuff,^{1,3} Antao Du,⁴ Andrew A. Maudsley,⁵
and Michael W. Weiner^{1,3,6}

Despite the continued spread of magnetic resonance imaging (MRI) methods in scientific studies and clinical diagnosis, MRI applications are mostly restricted to high-resolution modalities, such as structural MRI. While perfusion MRI gives complementary information on blood flow in the brain, its reduced resolution limits its power for detecting specific disease effects on perfusion patterns. This reduced resolution is compounded by artifacts such as partial volume effects, Gibbs ringing, and aliasing, which are caused by necessarily limited k -space sampling and the subsequent use of discrete Fourier transform (DFT) reconstruction. In this study, a Bayesian modeling procedure (K-Bayes) is developed for the reconstruction of perfusion MRI. The K-Bayes approach (described in detail in Part II: Modeling and Technical Development) combines a process model for the MRI signal in k -space with a Markov random field prior distribution that incorporates high-resolution segmented structural MRI information. A simulation study was performed to determine qualitative and quantitative improvements in K-Bayes reconstructed images compared with those obtained via DFT. The improvements were validated using in vivo perfusion MRI data of the human brain. The K-Bayes reconstructed images were demonstrated to provide reduced bias, increased precision, greater effect sizes, and higher resolution than those obtained using DFT.

KEY WORDS: Bayesian reconstruction, K-Bayes, Markov random field, perfusion MRI, structural MRI

INTRODUCTION

In vivo magnetic resonance imaging (MRI) of the human brain is proving to be a leading imaging modality for ascertaining the mechanisms of neurodegenerative disease progression such as Alzheimer's disease (AD), multiple sclerosis, and other brain diseases/injuries¹⁻⁴. To date, the primary application of MRI has been to determine disease-related anatomical changes observed using structural MRI. Consistent volumetric changes

have been detected that correlate with neurodegenerative disease, e.g., reduced hippocampal and entorhinal cortex volumes in AD³. In addition, a wide range of innovative and quantitative MRI measurements of cerebral perfusion, diffusion, metabolite concentrations, and neural activation promise to reveal functional changes that accompany neurodegenerative disease. An underutilized advantage of MRI over other imaging modalities is that a range of physiologic measurements can be obtained non-invasively for a single subject from the same scanner and during the same scanning session.

In particular, perfusion MRI provides a means to determine blood flow alterations in the human brain and potentially to detect effects specific to

¹From the Department of Radiology and Biomedical Imaging, University of California, San Francisco, 4150 Clement Street (114M), San Francisco, CA 94121, USA.

²From the Department of Epidemiology and Biostatistics, University of California, San Francisco, San Francisco, CA, USA.

³From the Department of Veterans Affairs Medical Center, 4150 Clement Street (114M), San Francisco, CA 94121, USA.

⁴From the Department of Neurology, Wayne State University, Detroit, MI, USA.

⁵From the Department of Radiology, University of Miami School of Medicine, Miami, FL, USA.

⁶From the Department of Medicine and Psychiatry, University of California, San Francisco, 4150 Clement Street (114M), San Francisco, CA 94121, USA.

Correspondence to: John Kornak, Department of Radiology and Biomedical Imaging, University of California, San Francisco, 4150 Clement Street (114M), San Francisco, CA 94121, USA; tel: +1-415-3534740; fax: +1-415-3539423; e-mail: john.kornak@ucsf.edu

Copyright © 2009 by The Author(s). This article is published with open access at Springerlink.com

Online publication 10 February 2009

doi: 10.1007/s10278-009-9183-y

particular brain diseases or injuries. However, the conventional reconstruction approach (for perfusion MRI) of discrete Fourier transform (DFT) is limited in terms of accuracy, precision, and resolution. These limitations lead to poor sensitivity and specificity when estimating the clinical effects of neurodegenerative diseases, psychiatric diseases, and brain injuries. There are two fundamentally different but related reasons why DFT produces reduced quality reconstructions. One reason is that the DFT reconstruction approach is unable to utilize complementary anatomical information available from high signal-to-noise-ratio (SNR) structural MRI. The second reason is that the limited SNR of perfusion MRI effectively restricts data acquisition to a small set of low spatial frequency signals, i.e., the center of “ k -space”. The K-Bayes reconstruction procedure deals effectively with these issues, thereby increasing the accuracy, precision, and resolution of perfusion MRI reconstructions. The K-Bayes model, DFT, and k -space are described in detail in Part II.

ASL Perfusion MRI

Arterial spin labeling (ASL) perfusion MRI (hereafter referred to as perfusion MRI) uses blood water as an endogenous tracer for cerebral blood flow. Perfusion MRI suffers from poor SNR because labeled blood water is only a tiny fraction (1–3%) of the overall MRI water signal from the brain. In order to compensate for the lower SNR, perfusion MRI is typically acquired with reduced spatial resolution compared with structural MRI. Perfusion MRI is typically acquired at a resolution of several millimeters compared to 1 mm for structural MRI; it therefore lacks positional (i.e., anatomical) specificity. An additional complication arises from the different perfusion values of gray matter and white matter. Perfusion of gray matter is usually two to three times higher than that of white matter⁵ and is close to zero in cerebrospinal fluid (CSF) and zero outside the brain. The poor spatial resolution of perfusion MRI introduces gray/white matter partial volume effects and, consequently, a bias towards lower perfusion estimates in gray matter close to white matter boundaries, complicating interpretation as to whether low perfusion reflects disease or is simply an artifact of the underlying tissue structure.

For these reasons, it is crucial to develop improved reconstruction methods capable of enhancing perfusion MRI image quality and resolution.

Advanced Bayesian (and Non-Bayesian) Reconstruction Approaches

While the conventional DFT method offers a convenient approach to reconstruct MRI data, it is considerably less sensitive to the phenomena we observe in perfusion MRI (i.e., blood flow) than those we observe in structural MRI. This deficiency calls for more sensitive reconstruction techniques such as those provided by Bayesian image analysis⁶, in particular the K-Bayes method proposed here.

Reconstruction procedures using Bayesian image analysis are already the norm in many areas of imaging (e.g., computer vision, motion tracking) and are starting to be applied increasingly in medical imaging^{7,8} and MRI^{9–12}. The art of Bayesian modeling is to develop prior models that characterize key aspects of available prior information to be combined with the information in the data. In fact, standard reconstruction methods based on likelihood theory (such as DFT) can (loosely) be thought of as a special case of a Bayesian model where there is no informative prior information.

The Bayesian formulation is particularly useful for combining information from multiple sources. There is a recent body of literature on combining information from different medical imaging modalities. Chen et al.¹³ provide a general method for fusing images from different modalities using an edge detection prior for identifying structural boundaries. The detection of edges between neighboring pixels turns off the a priori modeled smoothness between them (using Markov random fields, MRFs). This approach has spawned considerable research in applications to human brain imaging, in particular for emission computed tomography^{8,14,15}. Other methods have been developed specifically for improving MRI resolution using Bayesian image analysis. For example, Hurn et al.¹⁰ propose a simultaneous Bayesian reconstruction and tissue classification method that reconstructs multiple MRI modalities to a common high resolution. The tissue classification information is used to impose smoothness on the reconstruction through the use of MRFs. The approach is not specifically designed for the reconstruction of low-resolution k -space data (such as that from

perfusion MRI) and is not a “true” reconstruction approach in the sense that it is only applied to data after DFT. It is therefore subject to artifacts associated with DFT when applied to perfusion MRI. Miller et al.¹⁶ describe a likelihood-based method for reconstructing structural MRI from raw k -space data. However, the procedure was not designed to improve the reconstruction of low-resolution data and does not incorporate prior information. The method is extended in Schaeve and Miller¹⁷ to incorporate a MRF prior model that encourages smooth image reconstructions. However, this prior is limited by not varying smoothness levels according to whether neighboring voxels are of the same tissue type or not. Furthermore, images are only reconstructed to the same resolution that would be obtained by DFT. Denney and Reeves¹⁸ have developed a Bayesian approach for magnetic resonance spectroscopy imaging reconstruction (that could also be applied to other MRI modalities) that models the data in k -space and utilizes an edge-preserving prior. They use spectrally integrated estimates of the metabolites at each k -space point as raw data. However, the edge-preserving prior they adopt does not utilize tissue class information. A number of papers^{19–22} develop non-Bayesian approaches to improving the resolution of MRI data with tissue classification information. The basic idea is to utilize basis functions that are motivated by tissue classifications in order to smoothly represent signals within homogeneous tissue areas. Because it needs to be kept sparse (either by limiting the size of the basis set or by penalizing selection from a larger basis set), the basis function representation restricts the potential set of reconstructions.

To the best of the authors’ knowledge, the K-Bayes approach presented here represents the first attempt to combine a k -space signal modeling approach with a tissue classification prior within the Bayesian paradigm. The Bayesian approach provides a natural framework within which to balance the perfusion and anatomical information sources by quantifying them with probability distributions and combining them using Bayes’ theorem.

METHODS

Our K-Bayes reconstruction procedure aims to improve both spatial resolution and image quality

by overcoming the inherent limitations of DFT reconstruction. These improvements are achieved by incorporating high-resolution anatomical prior information to supply constraints for the physiological MR process while simultaneously relating the physiologic image to be reconstructed to the sampled k -space data points.

Incorporating Anatomical Information from Structural MRI (the Prior Distribution)

Structural MRI generates high-resolution maps that reveal local contrast between different types of tissue. These maps can be used to provide a priori anatomical constraints for the reconstruction of perfusion MRI. Structural MRI yields information at high spatial resolution owing to the abundance of water in the brain. The high density of free hydrogen in water generates good SNR and contrast-to-noise ratio (CNR). The human brain consists mostly of gray matter (neuronal cell bodies), white matter (axons), and CSF, which are distinguished readily with structural MRI due to differences in water concentration. The good CNR between these tissue types in structural MRI allows tissue classification of the corresponding anatomical information using available segmentation algorithms^{9,23–26}. The segmented anatomical image is employed as prior information for the K-Bayes reconstruction of perfusion MRI.

RESULTS

k -Space Simulation

Studies of simulated data were performed to compare K-Bayes with conventional DFT-based reconstruction approaches under controlled circumstances. Simulated datasets were generated using a version of the Montreal Neurological Institute (MNI) brain²⁷ that had been segmented into gray matter, white matter, and CSF at 128×128 resolution, along with the signal model developed in Part II of this paper. Figure 1 shows a simplified outline of how the data were simulated to mimic real perfusion MRI data.

The perfusion MRI signal was simulated with intensity in typical proportions of 2.5 (gray matter) to 1 (white matter)⁵. A relatively small and slowly varying quadratic spatial trend was

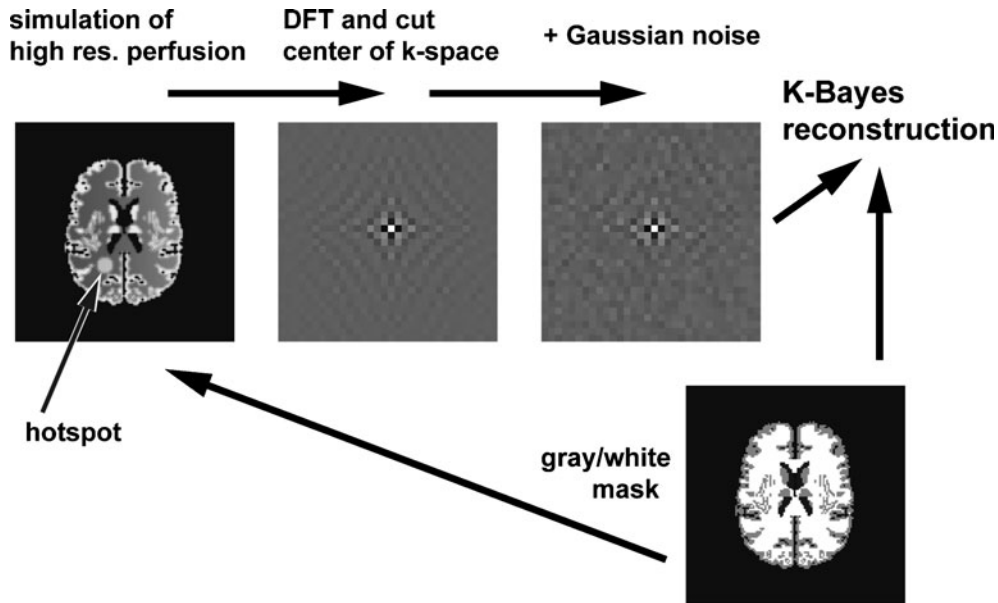


Fig 1. Procedure for generating simulated data. The high-resolution (128×128) gray/white matter segmented map was taken from the MNI dataset. Different levels of signal were generated within each tissue type; ratio of 2.5:1 gray/white. A hotspot plus a slight quadratic trend were added to the white matter and the whole map was spatially smoothed. The map was then transformed by DFT to k -space, Gaussian noise was added, and the center 32×32 region of k -space was cut out. This reduced k -space dataset formed the low-resolution simulated dataset used in the K-Bayes reconstruction along with the gray/white mask.

added to the white matter signal to provide smooth heterogeneity. Smoothing was also applied across the tissue boundaries to simulate a ‘bleeding effect’. Next, a hotspot of increased signal was added within the white matter region at a level equal to the original intensity of the white matter. The hotspot allowed testing of whether the prior information would cause the K-Bayes procedure to smooth away the effects of interest when they did not correspond to anatomical boundaries (i.e., to test whether K-Bayes was robust to information that did not match prior expectations). The resulting map was utilized as gold standard high-resolution data. To form raw k -space data, the map was discrete Fourier-transformed into k -space and the central 32×32 region was cut out (to simulate low-resolution data). Finally, simulated complex Gaussian noise was added to the data with a standard deviation corresponding to half the intensity of the white matter signal in image space. This noise level was chosen to produce a conservatively low SNR level with which to test K-Bayes. The simulated data had an average in-brain SNR level of 3.5, which should correspond to that of a typical

volume coil used for imaging at 1.5 Tesla²⁸. The simulated k -space and original segmentation data (i.e., tissue type information) became the input to the Bayesian algorithm. A conventional zero-filled DFT (zDFT) reconstruction was also obtained by placing the 32×32 k -space data at the center of a larger 128×128 array and filling with zeros elsewhere. This process was repeated for a Hamming windowed dataset, hereafter referred to simply as “Hamming”.

Statistical Metrics for Validation

To quantitatively evaluate K-Bayes reconstruction relative to zDFT, a range of statistical metrics were used. In order to set up the notation for the metrics, a gold standard image is defined to be y and an estimate of y (e.g., K-Bayes or zDFT) to be x . Then, for an image with N voxels, $i=1, \dots, N$, the metrics considered are:

1. Bias: $\frac{1}{N} \sum_{i=1}^N (y_i - x_i)$. This describes the average deviation from the truth, i.e., it determines whether there is a trend for the reconstruction to under- or overestimate. However, bias imparts no information about the magnitude of the deviations.

2. Root mean square error (RMSE):

$\sqrt{\frac{1}{N} \sum_{i=1}^N (y_i - x_i)^2}$. This estimate of the square root of the mean square residual size measures the average size of deviation from the truth.

3. Gray/white effect size:

$\frac{\bar{x}_G - \bar{x}_W}{\sqrt{\text{var}(x_G) + \text{var}(x_W)}/\sqrt{2}}$, where \bar{x}_G , $\text{var}(x_G)$ and \bar{x}_W , $\text{var}(x_W)$ are the mean and standard deviations of the signal of in gray and white matter voxels, respectively. This metric (closely related to CNR) quantifies the differentiability between the signals of gray and white matter. This metric has an advantage that it can be applied in the absence of a gold standard.

2D Simulation Results

Figure 2 shows the 128×128 true simulated perfusion map and the K-Bayes, zDFT, and Hamming reconstructions. There was considerable visual improvement in the K-Bayes reconstruction compared with zDFT. K-Bayes had increased definition and reduced ringing. The Hamming

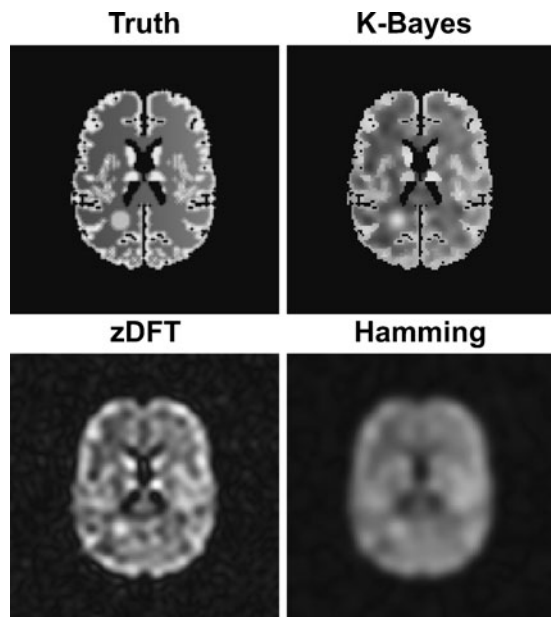


Fig 2. Results of reconstructions for 2D data: Truth (the high-resolution version of the simulated process in image space), K-Bayes, zDFT, and Hamming reconstructions. The K-Bayes reconstruction provided a visually improved representation of the truth compared with zDFT or Hamming.

reconstruction also reduces ringing compared with zDFT, but blurs the results, effectively reducing resolution.

Figure 3 displays the corresponding K-Bayes, zDFT, and Hamming windowed residuals from the truth. The real part of the noise was also added into the images to allow a comparison between the magnitude of the residual pattern and the noise level. The K-Bayes reconstruction exhibits visually reduced residual error compared to zDFT or Hamming. There is little or no visible pattern in the K-Bayes residuals, which blend into the noise. In contrast, the zDFT and Hamming residual patterns reveal considerable structure correlated with the true signal map that was obviously not captured by these reconstruction procedures.

Quantitative differences based on statistical metrics between K-Bayes, zDFT, and Hamming are given in Table 1. Hamming performed worse than K-Bayes and zDFT with respect to all metrics, except white matter bias where it performed better than zDFT but worse than K-Bayes. Therefore, only K-Bayes and zDFT results are further summarized here.

K-Bayes showed considerable improvement in gray and white matter bias compared with zDFT, implying that the levels in gray and white matter were more accurately reconstructed. In particular, notice that zDFT reduced the gray matter signal by 0.4 (a 15% signal loss), whereas with K-Bayes, the signal dropped by 0.05 (only a 2% signal loss). These reductions in bias are critically important for clinical perfusion studies where average changes across subjects in gray and white matter regions are assessed separately. There was approximately a 35% reduction in RMSE from 0.39 to 0.25 for the K-Bayes reconstruction relative to zDFT, and the gray/white effect size increased fourfold from 0.65 for zDFT to 2.42 for K-Bayes. K-Bayes performed better than zDFT with respect to RMSE in the hotspot, but not as well as zDFT with respect to hotspot bias. At first glance, it appears surprising that K-Bayes would do better in the hotspot with respect to any metric because the hotspot is a pattern not related to anatomical boundaries. However, zero filling in zDFT interpolates voxels in standard space and thus imposes smoothness constraints that may be more severe and extend over a larger and more arbitrarily determined region than those from the K-Bayes MRF prior. Furthermore, the improved reconstruction provid-

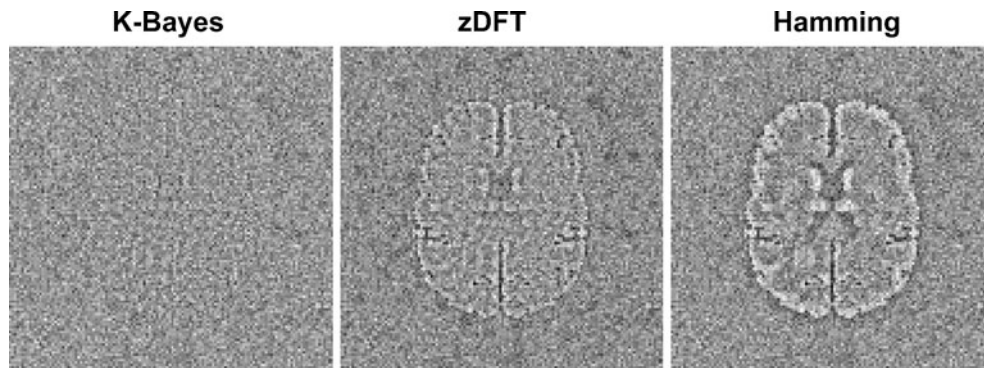


Fig 3. Maps of residuals from the high-resolution truth (with associated added noise). The K-Bayes residuals show reduced pattern relative to zDFT reconstruction, blending into the noise level. This implies that K-Bayes is performing considerably better than zDFT in fitting the true signal pattern.

ed by K-Bayes for areas where anatomical guidance is directly useful may indirectly help in other regions, thereby reducing RMSE in the hotspot; if part of the full perfusion signal has been correctly apportioned spatially, then there is less room for error in the non-anatomically related signal (e.g., that coming from the hotspot).

These results demonstrate that in the simplest 2D case, K-Bayes can quantifiably improve image quality over zDFT by increasing accuracy, precision, and resolution while simultaneously reducing artifacts (under the assumption that the a priori tissue constraints are correct).

3D Simulation

The 3D volume simulations were performed as for the 2D simulation except that the dataset consisted of multiple slices (representing multi-slice acquisition). The slices covered the complete MNI brain with four structural MRI slices corresponding to a single perfusion MRI slice.

The reconstructions of 3D K-Bayes and zDFT for the $128 \times 128 \times 128$ volume are displayed in Figure 4. Four adjacent slices of the high-resolution simulated truth are shown alongside the corresponding four reconstructed slices from K-Bayes and Hamming

windowed zDFT. The K-Bayes reconstruction not only provides much sharper definition than the zDFT reconstruction but also allows for variable changes in spatial pattern across the finer width MRI slices. For zDFT, the best that could be done was to interpolate the slices. Table 2 displays quantitative summaries for the 3D simulation study. Gray matter bias was reduced by 60% for K-Bayes compared with zDFT, though white matter bias was almost 50% higher in K-Bayes. Hamming had even better white matter bias than zDFT and K-Bayes, but considerably worse gray matter bias. The apparent improvement in white matter bias for the DFT-based approaches is likely artifactual, the chance consequence of two competing errors. First, there is a tendency for partial volume effects to merge signal between gray and white matter, thereby increasing the white matter level and reducing the gray. Second, the lack of signal outside the brain causes partial volume effects that reduce the white matter signal, to some degree canceling the first error. K-Bayes reduces the influence of the first partial volume effect because only light smoothness is modeled across gray/white boundaries. However, K-Bayes is not as susceptible to the second partial volume effect because of the strong prior modeling of a lack of signal in non-brain tissue. Thus, there is no competing error effect in K-

Table 1. Statistical Comparison of the Reconstruction Procedures for the 2D Simulated Perfusion MRI Reconstructions

	GM bias	WM bias	RMSE	Effect size	Hotspot bias	Hotspot RMSE
K-Bayes	-0.050	0.034	0.25	2.42	-0.083	0.19
zDFT	-0.406	0.057	0.39	0.65	-0.033	0.22
Hamming	-0.677	0.039	0.49	0.00	-0.320	0.34

Metrics of gray matter (GM) bias, white matter (WM) bias, RMSE, gray/white effect size, hotspot bias, and hotspot RMSE are presented for each reconstruction technique. K-Bayes provided the best results for all measures except hotspot bias

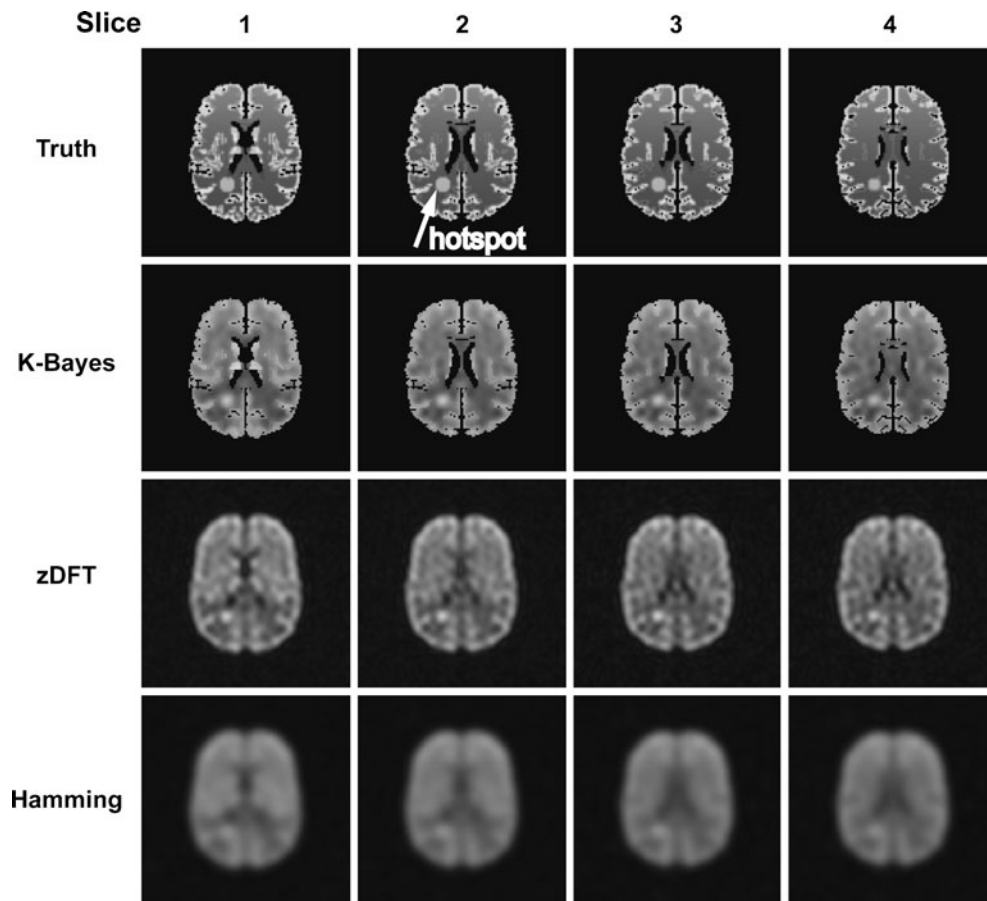


Fig 4. 3D simulations: true maps, K-Bayes, zDFT, and Hamming windowed zDFT reconstructions for a set of four slices at the higher-resolution of structural MRI. Visually, K-Bayes reconstruction does a much better job of reproducing the truth and nicely captures changes over the four slices.

Bayes. Furthermore, the RMSE drops from 0.47 for the DFT reconstruction down to 0.28 for the K-Bayes estimate, showing that K-Bayes reduced the “average” error by over 25%. The hotspot bias and RMSE were both considerably reduced with K-Bayes relative to zDFT or Hamming.

In summary, the simulation studies showed qualitatively and quantitatively that posterior estimates of maps based on maximizing the posterior distribution generally produced much improved

reconstructions over those obtained using zDFT. K-Bayes produced reconstructed images that better resembled the truth, with reduced Gibbs ringing and noise.

Real Perfusion MRI Reconstruction

K-Bayes reconstruction was performed on 4 Tesla perfusion MRI data to demonstrate feasibility in real applications. Figure 5 displays the procedures

Table 2. Statistical Comparison of the Reconstruction Procedures for the 3D Simulated Perfusion MRI Reconstructions

	GM bias	WM bias	RMSE	Effect size	Hotspot bias	Hotspot RMSE
K-Bayes	-0.25	0.119	0.28	1.69	-0.18	0.24
zDFT	-0.62	0.081	0.47	0.12	-0.22	0.30
Hamming	-0.78	0.033	0.56	0.28	-0.44	0.47

K-Bayes provided the best results for all measures except WM bias

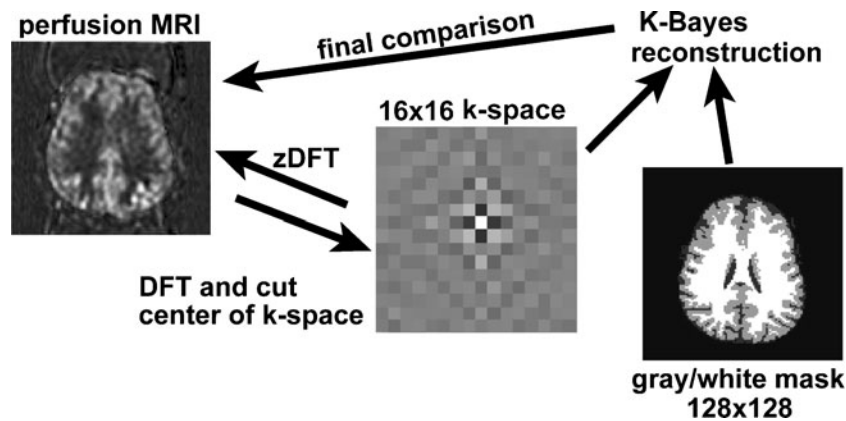


Fig 5. Real perfusion MRI analysis: high-resolution (32×64) perfusion MRI map is discrete Fourier-transformed into k -space and the center 16×16 region is cut out. The reduced k -space data are reconstructed using K-Bayes to high resolution (128×128). The K-Bayes reconstruction is then compared with a zDFT reconstruction from the 16×16 data. Gold standard is the 32×64 perfusion MRI map interpolated to 128×128 .

used to perform and evaluate the different reconstruction techniques. Institutional Review Board approval had been obtained for this data which was acquired as part of a larger study.

The original perfusion data were acquired with 32×64 resolution using a continuous ASL sequence, were zero-filled to 128×128 , and inverse discrete Fourier-transformed to generate a pseudo-gold standard map. zDFT was then applied to the pseudo-gold standard magnitude map, providing zero-filled and phase-corrected k -space data. The central 16×16 region was then cut out to create a reduced resolution k -space dataset. A simultaneously acquired 128×128 structural MRI was registered and re-sliced to match the perfusion data. The co-registered structural MRI was then segmented into gray matter, white matter, and CSF for input into K-Bayes. The 16×16 perfusion MRI dataset was reconstructed using K-Bayes, zDFT, and Hamming. Each reconstruction was then compared to the gold standard using the statistical metrics of bias, RMSE, and gray/white effect size.

The results of the different reconstructions are shown in Figure 6. K-Bayes clearly provides the best visual reconstruction of the three approaches. It presents the most contrast and captures more of the gold standard structure. The numerical comparisons in Table 3 indicate that K-Bayes improves over the other methods for all metrics. In particular, bias is around one fourth of that for zDFT, and the gray/white effect size is 50% higher. The RMSE did not show the level of improvements for K-Bayes that were observed in the simulation

studies. We believe that there are two reasons for this. First the (pseudo) gold standard is expanded via zero filling from a small enough region of k -space such that it contains artifacts of Gibbs ringing and aliasing. K-Bayes reconstruction of the further reduced dataset does not reproduce these artifacts, whereas the zDFT reconstruction does. Therefore, the RMSE of zDFT would increase and that of K-Bayes would decrease when

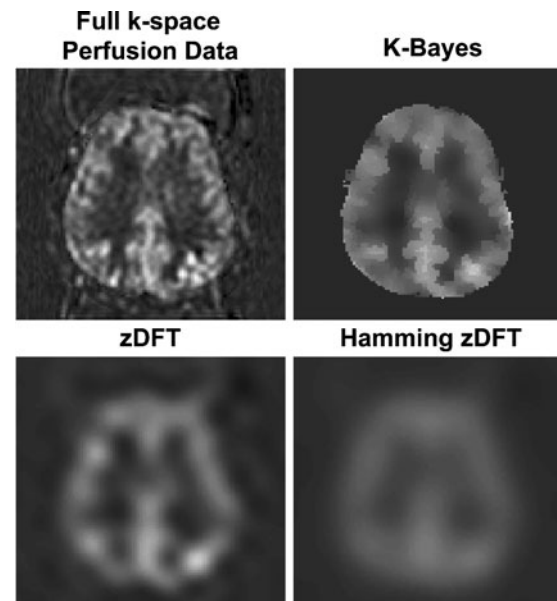


Fig 6. Reconstructions from K-Bayes, zDFT, and zDFT of Hamming windowed data. K-Bayes provides the most detailed reconstruction and recaptures many higher resolution features lost in the DFT-based reconstruction.

Table 3. Statistical Comparison of the Reconstruction Procedures for the Real Perfusion MRI Reconstructions

	GM bias	WM bias	RMSE	Effect size
K-Bayes	-0.009	0.006	0.108	1.7
zDFT	-0.038	0.022	0.110	1.3
Hamming	-0.150	0.050	0.140	0.8

K-Bayes provided the best results for all measures: having the smallest bias, RMSE, and largest effect size

compared to a true gold standard that did not contain Gibbs ringing and aliasing artifacts. Second, K-Bayes reduces noise that exists in the gold standard. Unlike the simulation study, the gold standard here contains noise. A definitive evaluation would require high-resolution and low-noise perfusion MRI to be used as a gold standard, but this is currently not available as a standard acquisition procedure.

Computation Time

Computation was performed with a Dell Precision 370 desktop computer running RedHat Enterprise Linux 4.0 on a single 3.20 GHz Pentium 4 processor using c-code. Complete convergence of the EM algorithm (to machine tolerance) for single slice data required less than 1 h. Three-dimensional reconstruction took on the order of 1 day to reach reasonable convergence (i.e., there were no fundamental differences in the reconstruction or statistical metrics if the algorithm was continued). These reconstruction times can be drastically reduced through parallelization, which is computationally trivial for the EM procedure. We found that parallelization yields almost linear speed up with the number of processors.

Discussion

Although perfusion MRI has great potential for aiding clinical applications including diagnosis and surgical intervention, it has not been attainable with the high SNR of structural MRI. Hence, perfusion MRI has necessarily been acquired at low spatial resolution, limiting its scientific and clinical application. The K-Bayes reconstruction procedure boosts the effective resolution of perfusion MRI by utilizing information from the high-resolution structural MRI. K-Bayes capitalizes on the knowledge that the perfusion process is to some degree constrained to the same tissue

boundaries visible with high-resolution structural MRI.

The simulation studies and real data analysis presented here have shown that posterior estimates of maps based on maximizing the posterior distribution yielded much improved reconstructions over those obtained using standard DFT methods. The K-Bayes reconstructions better resembled the truth, with much reduced Gibbs ringing and noise and improved statistical metrics. The improved accuracy, precision, and resolution afforded by K-Bayes reconstruction has the potential to push perfusion MRI into mainstream research of neurodegenerative and other brain diseases, providing significant advances in diagnosis and treatment evaluation. There is evidence to believe that perfusion effects precede structural effects in neurodegenerative disease progression²⁹. Therefore, perfusion MRI could find applications as a biomarker for treatment effects in early disease as well as ultimately provide a method for early disease detection and screening.

Additional steps are needed before K-Bayes can be used routinely for perfusion MRI reconstruction. First, the robustness of K-Bayes to segmentation errors and to misregistration between structural and perfusion scans need to be assessed. The co-registration and segmentation of brain MRI are imperfect procedures in which errors inevitably occur. Quality control guidelines need to be developed that incorporate acceptable levels of misregistration and segmentation error. Furthermore, K-Bayes prior models could be developed with increased flexibility to account for registration segmentation uncertainty.

Secondly, known perfusion effects across populations need to be validated and demonstrated to be observable with improved statistical power. This will require the validation of K-Bayes against specially acquired high-resolution gold standard datasets and application of K-Bayes to one or more large clinical studies. These points are the focus of ongoing work by the authors.

ACKNOWLEDGMENTS

This work was supported by a Society for Imaging Informatics in Medicine (SIIM) research grant; NIH grants R01 NS41946, R01 AG010897, R01 AG012435, P41 RR023953; and the San Francisco Veterans Affairs Medical Center Medical Research Service. We thank Bill Chu for helpful comments and suggestions in the preparation of this manuscript.

OPEN ACCESS

This article is distributed under the terms of the Creative Commons Attribution Noncommercial License which permits any noncommercial use, distribution, and reproduction in any medium, provided the original author(s) and source are credited.

REFERENCES

- Mueller SG, et al.: The Alzheimer's disease neuroimaging initiative. *Neuroimaging Clin N Am* 15:869–877, 2005; xi–xii
- Mueller SG, et al.: Ways toward an early diagnosis in Alzheimer's disease: The Alzheimer's Disease Neuroimaging Initiative (ADNI). *Alzheimers Dement* 1:55–66, 2005
- Du AT, et al.: Higher atrophy rate of entorhinal cortex than hippocampus in AD. *Neurology* 62:422–427, 2004
- Jack Jr., CR, et al.: Comparison of different MRI brain atrophy rate measures with clinical disease progression in AD. *Neurology* 62:591–600, 2004
- Roberts DA, Detre JA, Bolinger L, Insko EK, Leigh Jr., JS: Quantitative magnetic resonance imaging of human brain perfusion at 1.5 T using steady-state inversion of arterial water. *Proc Natl Acad Sci U S A* 91:33–37, 1994
- Besag JE: Towards Bayesian image analysis. *J Appl Stat* 16:395–407, 1989
- Green PJ: Bayesian reconstructions from emission tomography data using a modified EM algorithm. *IEEE Trans Med Imag* 9:84–93, 1990
- Ouyang X, Wong WH, Johnson VE, Hu X, Chen C-T: Incorporation of correlated structural images in PET image reconstruction. *IEEE Trans Med Imag* 13:627–640, 1994
- Zhang Y, Brady M, Smith S: Segmentation of brain MR Images through a hidden Markov random field model and the expectation maximization algorithm. *IEEE Trans Med Imag* 20:45–57, 2001
- Hum MA, Mardia KV, Hainsworth TJ, Kirkbridge J, Berry E: Bayesian fused classification of medical images. *IEEE Trans Med Imag* 15:850–858, 1996
- Raj A, et al.: Bayesian parallel imaging with edge-preserving priors. *Magn Reson Med* 57:8–21, 2007
- Woolrich MW, Behrens TE, Beckmann CF, Smith SM: Mixture models with adaptive spatial regularization for segmentation with an application to fMRI data. *IEEE Trans Med Imag* 24:1–11, 2005
- Chen C-T, Ouyang WH, Wong XH, Johnson VE: Sensor fusion in image reconstruction. *IEEE Trans Nucl Sci* 38:678–692, 1991
- Bowsher JE, Johnson VE, Turkington TG, Jaszczak RJ, Floyd Jr., CE, Coleman RE: Bayesian reconstruction and use of anatomical a priori information for emission tomography. *IEEE Trans Med Imag* 15:673–686, 1996
- Sastry S, Carson RE: Multimodality Bayesian algorithm for image reconstruction in positron emission tomography: a tissue composition model. *IEEE Trans Med Imag* 16:750–761, 1997
- Miller IM, Schaewe TJ, Cohen SB, Ackerman JH: Model-based maximum-likelihood estimation for phase- and frequency-encoded magnetic-resonance-imaging data. *J Magn Reson, Ser B* 107:210–221, 1995
- Schaewe TJ, Miller IM: Parallel algorithms for maximum a posteriori estimation of spin density and spin-spin decay in magnetic resonance imaging. *IEEE Trans Med Imag* 14:362–373, 1995
- Denney Jr. TS, Reeves SJ: Bayesian image reconstruction from Fourier-domain samples using prior edge information. *J Electron Imaging* 14:043009, 043001–043011, 2005
- Hu X, Levin DN, Lauterbur PC, Spraggins T: SLIM: spectral localization by imaging. *Magn Reson Med* 8:314–322, 1988
- Liang ZP, Lauterbur PC: A generalized series approach to MR spectroscopic imaging. *IEEE Trans Med Imaging* 10:132–137, 1991
- Liang ZP, Lauterbur PC: An efficient method for dynamic magnetic resonance imaging. *IEEE Trans Med Imaging* 13:677–686, 1994
- Jacob M, Zhu X, Ebel A, Schuff N, Liang ZP: Improved model-based magnetic resonance spectroscopic imaging. *IEEE Trans Med Imaging* 26:1305–1318, 2007
- Ashburner J, Friston KJ: Multimodal image coregistration and partitioning—A unified framework. *NeuroImage* 6:209–217, 1997
- Prince JL, Pham D, Tan O: Optimization of MR pulse sequences for Bayesian image segmentation. *Med Phys* 22:1651–1656, 1995
- Pham DL, Xu C, Prince JL: Current methods in medical image segmentation. *Annu Rev Biomed Eng* 2:315–337, 2000
- Pham DL, Prince JL: Adaptive fuzzy segmentation of magnetic resonance images. *IEEE Trans Med Imaging* 18:737–752, 1999
- Cocosco CA, Kollokian V, Kwan RK-S, Evans AC: BrainWeb: Online interface to a 3D MRI simulated brain database. *Proceedings of 3rd International Conference on Functional Mapping of the Human Brain, Canada, 1997*
- Wang Z, Wang J, Connick TJ, Wetmore GS, Detre JA: Continuous ASL (CASL) perfusion MRI with an array coil and parallel imaging at 3T. *Magn Reson Med* 54:732–737, 2005
- Hayasaka S, et al.: A non-parametric approach for co-analysis of multi-modal brain imaging data: application to Alzheimer's disease. *Neuroimage* 30:768–779, 2006